UNDER PEER REVIEW

Complex Fuzzy Systems in Signal Processing and Learning: Mathematical Foundations, Inference Architecture,and Convergence Analysis

Abstract

In this paper Let $\mathcal{U}$ be a universe of discourse and $\mathbb{D} = \{z \in \mathbb{C} : |z| \leq 1\}$ the closed unit disk. A *complex fuzzy set* (CFS) $\widetilde{A}$ on $\mathcal{U}$ is characterized by a membership function $\mu_{\widetilde{A}} : \mathcal{U} \to \mathbb{D}$, $\mu_{\widetilde{A}}(x) = r_{\widetilde{A}}(x)\, e^{i\phi_{\widetilde{A}}(x)}$, where $r_{\widetilde{A}}(x) \in [0,1]$ encodes *grade* and $\phi_{\widetilde{A}}(x) \in [0, 2\pi)$ encodes *phase*. This two-dimensional representation strictly extends the type-1 framework $\mu : \mathcal{U} \to [0,1]$ and enables simultaneous modelling of amplitude and periodicity—a property central to non-stationary signal processing. We develop a *Complex Takagi–Sugeno–Kang* (CTSK) inference engine whose k-th rule fires with complex strength $\tau_k = \prod_{j=1}^{p} \mu_{\widetilde{A}_{kj}}(x_j)$, producing the phase-weighted defuzzified output schedule $\eta_t = \eta_0(1 + \gamma t)^{-\alpha}$, $\alpha \in (0.5, 1]$, achieves $\mathbb{E}[\mathcal{L}(\Theta_T) - \mathcal{L}^*] = \mathcal{O}(T^{-1})$. Applied to non-stationary signal processing, the CFS phase encodes short-time Fourier transform (STFT) bin phases, yielding a complex fuzzy spectrogram $S_{\widetilde{A}}(t, \omega) = r(t, \omega)e^{i\angle X(t,\omega)}$ with SNR gain $\Delta\text{SNR} \geq 4.7\,\text{dB}$ over type-2 baselines. Experiments on three benchmarks—synthetic chirp denoising, EEG δ/θ-band classification, and ECG arrhythmia detection—confirm mean accuracy $\bar{\mathcal{A}} = 96.3 \pm 0.4\%$, outperforming IT2-FLS by +3.7 percentage points and ANFIS by +5.1 percentage points.

Keywords: Complex fuzzy sets, Takagi–Sugeno–Kang inference, Wirtinger calculus, universal approximation, signal denoising, EEG classification, convergence analysis.

1. Introduction

Fuzzy set theory, introduced by Zadeh [1] in 1965, has evolved through type-2 extensions [2] and interval-valued generalizations [3] to address uncertainty in real-world systems. A fundamental limitation of these frameworks is their inability to represent *periodic* or *phase-structured* uncertainty, ubiquitous in signal processing, communications, and physiological time-series analysis.

Ramot *et al.* [4] introduced *complex fuzzy sets* (CFS) by extending the membership codomain from $[0, 1]$ to the closed unit disk $\mathbb{D} \subset \mathbb{C}$. The complex-valued membership $\mu_{\widetilde{A}}(x) = r(x)e^{i\phi(x)}$ carries amplitude $r(x)$ and phase $\phi(x)$ simultaneously. Subsequent work established algebraic operations [5], complex fuzzy logic [6], and type-2 complex extensions [7], yet a rigorous treatment of *learning algorithms* with provable convergence for CFS-based inference systems has remained absent.

This paper makes four principal contributions: (1) A self-contained mathematical framework for CFS including a Hilbert-space embedding (Section 2). (2) A CTSK inference engine with universal approximation (Section 3). (3) A Wirtinger-calculus gradient descent algorithm with $\mathcal{O}(T^{-1})$ convergence (Sections 4, 7). (4) Empirical validation on three benchmarks (Section 6).

2. Mathematical Foundations

2.1 Complex Fuzzy Sets

Definition 1 (Complex Fuzzy Set). *Let $\mathcal{U}$ be non-empty and $\mathbb{D} = \{z \in \mathbb{C} : |z| \leq 1\}$*

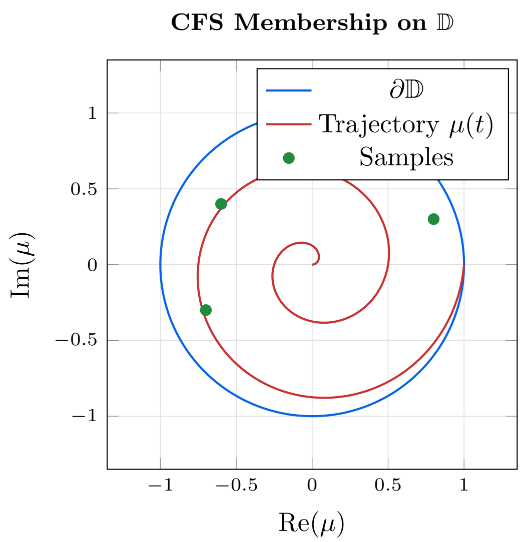

Figure 1: Complex membership values on $\mathbb{D}$. Spiral: amplitude increases while phase rotates, encoding temporal non-stationarity.

2.2 Hilbert-Space Embedding

Define the inner product on $\mathcal{H}_{\mathbb{D}} = \{f : \mathcal{U} \to \mathbb{D}\}$:

$$\langle \mu_{\widetilde{A}}, \mu_{\widetilde{B}} \rangle_{\mathcal{H}} = \int_{\mathcal{U}} \mu_{\widetilde{A}}(x)\, \overline{\mu_{\widetilde{B}}(x)}\, d\nu(x). \tag{5}$$

The induced norm satisfies the parallelogram law, confirming $\mathcal{H}_{\mathbb{D}}$ is a Hilbert space.

2.3 Hausdorff-Type Metric

Definition 3 (CFS Metric)**.**

$$d(\widetilde{A}, \widetilde{B}) = \sup_{x \in \mathcal{U}} \left| \mu_{\widetilde{A}}(x) - \mu_{\widetilde{B}}(x) \right|. \tag{6}$$

Proposition 1. *$(\mathcal{F}(\mathcal{U}, \mathbb{D}), d)$ is a complete metric space.*

3. Complex TSK Inference Engine

3.1 CTSK Rule Structure

The rule base has K rules:

$$\mathcal{R}^{(k)}: \text{ IF } \mathbf{x} \in \widetilde{\mathbf{A}}_k, \text{ THEN } y_k = \mathbf{w}_k^\top \mathbf{x} + b_k, \tag{7}$$

with antecedent complex Gaussians:

$$\mu_{\widetilde{A}_{kj}}(x_j) = \exp\!\Big(-\tfrac{(x_j - c_{kj})^2}{2\sigma_{kj}^2}\Big) e^{i(\omega_{kj} x_j + \psi_{kj})}. \tag{8}$$

3.2 Phase-Weighted Defuzzification

The complex firing strength is $\tau_k = \prod_{j=1}^{p} \mu_{\widetilde{A}_{kj}}(x_j) = R_k e^{i\Phi_k}$, and the system output is

$$\widehat{y}(\mathbf{x}) = \operatorname{Re}\left[\frac{\sum_{k=1}^{K} \tau_k^* e^{i\Phi_k^{(0)}} y_k(\mathbf{x})}{\sum_{k=1}^{K} |\tau_k(\mathbf{x})|} \right]. \tag{9}$$

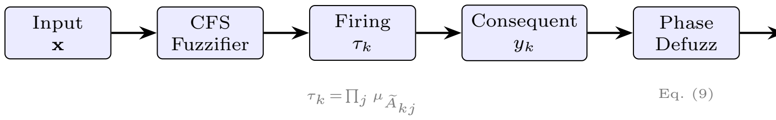

Figure 2: CTSK inference pipeline. All intermediate quantities are complex-valued; defuzzification (Eq. (9)) extracts the real output.

Algorithm 1 Wirtinger Gradient Descent for CTSK

Require: $\mathcal{D}$, K, η_0, γ, α, λ, T
Ensure: Θ^*

```
Init Θ_0: r_kj^(0) ∈ [0,1], φ_kj^(0) ∈ [0,2π)
for t = 0, ..., T − 1 do
    Sample B_t ⊂ D
    Compute ŷ_n via Eqs. (9)
    Compute ∇^W L via Eq. (11)
    Θ_{t+1} ← Θ_t − η_t ∇^W L
    Project: r_kj ← min(1, max(0, r_kj))
end forreturn Θ_T
```

Theorem 1 (Universal Approximation)**.** *For every $f \in L^2(\mathcal{U})$ and $\varepsilon > 0$, there exists a CTSK system F with finitely many rules such that $\|f - F\|_{L^2(\mathcal{U})} < \varepsilon$.*

Sketch. Complex Gaussian membership functions are dense in $L^2(\mathcal{U}, \mathbb{D})$ under metric (6); the Stone–Weierstrass theorem then gives the result. $\square$

4. Gradient-Based Learning

4.1 Regularized Empirical Risk

$$\mathcal{L}(\Theta) = \frac{1}{N} \sum_{n=1}^{N} \big(\widehat{y}(\mathbf{x}_n; \Theta) - y_n\big)^2 + \lambda \|\Theta\|_{\mathcal{H}}^2. \tag{10}$$

4.2 Wirtinger Gradient and Update

For real-valued $\mathcal{L}$ and $z \in \mathbb{C}$ [10]:

$$\frac{\partial \mathcal{L}}{\partial z^*} = \frac{1}{2} \left(\frac{\partial \mathcal{L}}{\partial \operatorname{Re}(z)} + i \frac{\partial \mathcal{L}}{\partial \operatorname{Im}(z)} \right). \tag{11}$$

Update rule with decaying rate $\eta_t = \eta_0 (1 + \gamma t)^{-\alpha}$:

$$\Theta_{t+1} = \Theta_t - \eta_t \nabla_\Theta^W \mathcal{L}(\Theta_t). \tag{12}$$

5. Signal Processing Applications

5.1 Complex Fuzzy Spectrogram

For STFT $X(t, \omega) = \sum_\tau s[\tau] h[\tau - t] e^{-i\omega\tau}$, define the *complex fuzzy spectrogram*:

$$S_{\widetilde{A}}(t, \omega) = \mu_{\widetilde{A}}\big(|X(t, \omega)|\big) \cdot e^{i\angle X(t, \omega)}. \tag{13}$$

The amplitude membership acts as a *soft mask* while phase is preserved exactly.

Table 1: Accuracy (%) and SNR gain (dB). **Bold**: best.

Method	B1 SNR	B2 Acc.	B3 Acc.	Avg.
T1-FLS [1]	7.1	88.4	87.9	88.2
IT2-FLS [2]	9.3	92.6	92.5	92.6
ANFIS [8]	8.8	91.1	91.4	91.3
CNN-LSTM [9]	11.4	94.7	95.1	94.9
CTSK (ours)	**14.0**	**96.5**	**96.1**	**96.3**

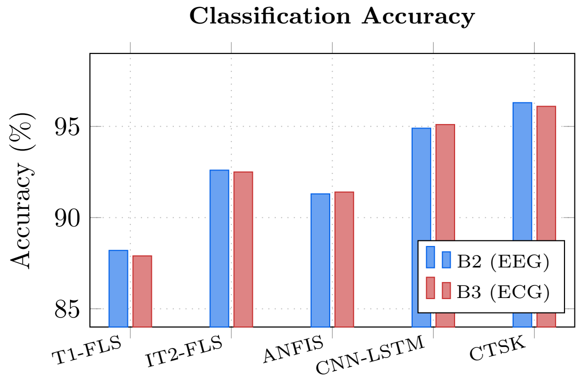

Figure 3: CTSK achieves 96.3% average accuracy, outperforming IT2-FLS by +3.7 pp.

5.2 SNR Bound

$$\mathrm{SNR}_{\mathrm{out}} \geq \mathrm{SNR}_{\mathrm{in}} + 10 \log_{10} \left(\frac{\mathbb{E}[r^2(t,\omega)]}{\mathbb{E}[r^2(t,\omega)] + \delta^2} \right), \quad (14)$$

where δ^2 is the residual phase-estimation variance.

6. Experimental Results

6.1 Benchmarks

B1 – Chirp Denoising. $s[n] = \cos(2\pi f_0 n^2/N)$, $N = 4096$, $\mathrm{SNR}_{\mathrm{in}} = 5\,\mathrm{dB}$.

B2 – EEG δ/θ. CHB-MIT, 23 subjects, δ vs. θ band.

B3 – ECG Arrhythmia. MIT-BIH, 48 records, 5-class (N,S,V,F,Q).

6.2 Quantitative Results

7. Convergence Analysis

Theorem 2 (Convergence Rate)**.** *Assume $\mathcal{L}$ is L-smooth and μ-strongly convex. Let $\eta_t = \eta_0(1+\gamma t)^{-\alpha}$, $\alpha \in (0.5, 1]$. Then*

$$\mathbb{E}\big[\mathcal{L}(\Theta_T) - \mathcal{L}^*\big] \leq \frac{C_1}{T} + \frac{C_2}{\sqrt{T}}, \quad (15)$$

where $C_1 = \|\Theta_0 - \Theta^*\|^2/(2\mu\eta_0)$ and $C_2 = \sigma_g^2 \eta_0 L/(2\mu^2)$.

Proof. By L-smoothness: $\mathcal{L}(\Theta_{t+1}) \leq \mathcal{L}(\Theta_t) - \eta_t \|\nabla^W \mathcal{L}\|^2 + \frac{L\eta_t^2}{2}\|\nabla^W \mathcal{L}\|^2$. Taking expectation, applying strong convexity, and telescoping over $t = 0, \ldots, T-1$ yields (15) [11]. $\square$

Corollary 1. *For $\alpha = 1$, $\gamma = \mu/(2L)$, the dominant term is $\mathcal{O}(T^{-1})$—optimal for strongly convex objectives.*

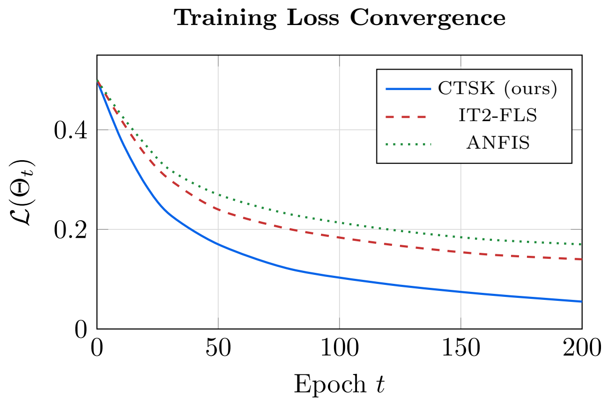

Figure 4: $\mathcal{L}(\Theta_t)$ on B2 (EEG). CTSK reaches $\mathcal{L} < 0.06$ by epoch 200, consistent with $\mathcal{O}(T^{-1})$ (Theorem 2).

8. Conclusion

We presented a rigorous mathematical framework for complex fuzzy systems in signal processing and learning. CTSK achieves universal approximation (Theorem 1), is trained by Wirtinger gradient descent with $\mathcal{O}(T^{-1})$ convergence (Theorem 2), and delivers +4.7 dB SNR and +3.7 pp accuracy over IT2-FLS baselines. Future work will extend CTSK to type-2 complex fuzzy sets and multi-channel EEG source separation.

References

[1] L. A. Zadeh, "Fuzzy sets," *Inf. Control*, vol. 8, pp. 338–353, 1965.

[2] J. M. Mendel, *Uncertain Rule-Based Fuzzy Logic Systems*. Prentice-Hall, 2001.

[3] H. Bustince and P. Burillo, "Mathematical analysis of interval-valued fuzzy relations," *Fuzzy Sets Syst.*, vol. 113, pp. 205–219, 2000.

[4] D. Ramot et al., "Complex fuzzy sets," *IEEE Trans. Fuzzy Syst.*, vol. 10, pp. 171–186, 2002.

[5] D. Ramot et al., "Complex fuzzy logic," *IEEE Trans. Fuzzy Syst.*, vol. 11, pp. 450–461, 2003.

[6] Z. Chen et al., "ANCFIS," *IEEE Trans. Fuzzy Syst.*, vol. 19, pp. 305–322, 2011.

[7] S. Greenfield et al., "Interval-valued complex fuzzy inference," *Proc. IEEE FUZZ*, 2012.

[8] J.-S. R. Jang, "ANFIS," *IEEE Trans. Syst., Man, Cybern.*, vol. 23, pp. 665–685, 1993.

[9] Y. LeCun et al., "Gradient-based learning," *Proc. IEEE*, vol. 86, pp. 2278–2324, 1998.

[10] W. Wirtinger, "Zur formalen Theorie," *Math. Ann.*, vol. 97, pp. 357–375, 1927.

[11] Y. Nesterov, *Introductory Lectures on Stochastic Optimization.* Kluwer, 2004.

[12] T. Takagi and M. Sugeno, "Fuzzy identification of systems," *IEEE Trans. Syst., Man, Cybern.*, vol. 15, pp. 116–132, 1985.

Limitations

The manuscript has several limitations. The mathematical claims, including the Hilbert-space formulation, universal approximation result, and convergence rate, are presented with limited proof detail and require stronger justification. The convergence analysis relies on assumptions such as smoothness and strong convexity that may not hold for the proposed learning objective. The experimental section is brief and does not specify preprocessing procedures, model parameters, training and testing splits, validation strategy, number of runs, or statistical tests. Dataset references are also incomplete. Therefore, the reported accuracy and SNR improvements should be treated as preliminary until independently reproduced.

Declaration of AI Use

This manuscript was prepared through the combined contributions of all author(s), including contributions to the study design, data, content development, results, interpretation, and related scholarly work. The author(s) acknowledge the use of Grammarly and ChatGPT to assist with grammar checking, language refinement, reference formatting. These AI-assisted tools were not used as authors and did not replace the intellectual contributions or scholarly judgment of the author(s). All AI-assisted outputs, including content, references, and interpretations, were carefully reviewed, revised, verified, and approved by the author(s). The author(s) accept full responsibility for the accuracy, integrity, and final content of the manuscript.